

Notes

Mesomorphic Form of Syndiotactic Polypropylene

Vittoria Vittoria and Liberata Guadagno

Dipartimento di Ingegneria Chimica e Alimentare, Università di Salerno, via Ponte Don Melillo, Fisciano (Salerno), Italy

Angiolina Comotti and Roberto Simonutti

Dipartimento di Scienza dei Materiali, Università di Milano, via Emanueli, 15, 20126 Milano, Italy

Finizia Auriemma* and Claudio De Rosa

Dipartimento di Chimica, Università degli Studi di Napoli "Federico II", via Mezzocannone, 4, 80134 Napoli, Italy

Received March 1, 2000

Revised Manuscript Received April 22, 2000

Introduction

Syndiotactic polypropylene (sPP) presents a very complex polymorphic behavior.^{1–10} Four crystalline forms of sPP have been described so far. Forms I and II are characterized by chains in $(T_2G_2)_n$ helical conformation, whereas forms III and IV present chains in trans planar^{3,9} and $(T_6G_2T_2G_2)_n$ ¹⁰ conformations, respectively.

Form I is the stable form of sPP obtained under the most common conditions of crystallization (melt and solution crystallization) in powder samples and single crystals of sPP.^{4–7,11}

Form II is obtained by stretching at room temperature compression molded specimens of sPP samples having low stereoregularity.^{8,12} If the most stereoregular samples obtained with homogeneous metallocene-based catalysts are stretched, fibers in the *trans*-planar form III are obtained. However, also for highly stereoregular sPP samples, the pure form II may be obtained upon release of the tension in fibers initially in the *trans*-planar form III.¹² Under these conditions, a phase transition from form III to the isochiral form II occurs.^{12,13} Annealing fiber samples of form II or form III at high temperatures (100 °C) gives fibers with a mixture of crystals of forms I and II.⁸

Form III is known as the metastable polymorph of sPP. Independent of the stereoregularity of sPP samples, form III is obtained through cold drawing procedures of sPP samples quenched from the melt into ice–water mixtures.⁹

Finally, form IV is obtained upon exposure to solvent vapors (e.g., benzene, toluene) of sPP fiber samples initially in form III.¹⁰

In a recent paper by Nakaoki et al.,¹⁴ the crystallization of the *trans*-planar form III is reported to be spontaneously induced at 0 °C without any mechanical stress. The solid state ¹³C NMR spectra recorded at room temperature for sPP films of a highly stereoregular

sPP sample, quenched at 0 °C from the melt, indicate that the amount of nuclei in *trans*-planar conformational environment embedded in rigid regions of the samples, increase with the increasing of the time the sPP films are kept at 0 °C. More precisely sPP samples immediately taken out from the bath at 0 °C, rapidly crystallize in the more stable T_2G_2 helical forms, at room temperature. Longer permanence times at 0 °C of these films increase the number of long chain stretches in the *trans*-planar conformation which inhibit the crystallization of the sample into the more stable form I at room temperature.

The X-ray diffraction pattern recorded at room temperature of the sPP sample kept at 0 °C for long time shows a broad peak centered around $2\theta = 17^\circ$ with a shoulder around $2\theta = 24^\circ$ and cannot be identified with the normal profile of an amorphous sPP sample.⁸ Nakaoki et al.¹⁴ identify the two bumps centered at $2\theta = 17^\circ$ and 24° with the (002) and the (020) + (110) reflections, respectively, of form III of sPP.⁹ This indexing is clearly wrong; the structural model proposed by Chatani et al. for the form III of sPP, indeed, is characterized by chains in an orthorhombic lattice, centered on the C-face, with $a = 5.22 \text{ \AA}$, $b = 11.17 \text{ \AA}$, and $c = 5.06 \text{ \AA}$.⁹ We also notice that the most intense diffraction peaks of form III occur at different 2θ positions from those of the sample in question, i.e., $2\theta = 15.9$ and 18.8° (Cu K α , Miller indices 020 and 110⁹). Of course, a reduced size of the crystallites could produce the broadening of these crystalline peaks, leading them to coalesce into a single one with a maximum placed midway (i.e., around $2\theta = 17^\circ$) in the limit of very small sizes. The half-height width of the diffraction peak thus resulting would span more than 5° of 2θ , in a 2θ range comprising between 15 and 20° . The presence of an amorphous contribution (with a maximum centered around $2\theta = 16^\circ$) would broaden even more the resulting diffraction halo. In the X-ray diffraction profile of Figure 3a of ref 14, resulting from this novel phase of sPP plus an amorphous contribution, the maximum centered around $2\theta = 17^\circ$ spans only 4° of 2θ and the diffraction intensity already falls off at $2\theta = 19^\circ$, position corresponding to the most intense diffraction peak of form III.⁹ Hence, although this new phase is correctly characterized by the authors of ref 14, as containing long strands of chains in *trans*-planar conformation, it can be identified neither with form III nor with any single other known crystalline polymorph of sPP.

In this paper, the nature of this new phase is investigated, applying several different experimental techniques on sPP samples suitably prepared according to the procedure suggested by Nakaoki et al.¹⁴ The phase transformations of the sPP samples in this new form with the temperature are also studied.

Table 1. Solid State NMR Chemical Shift (CS) and Spin–Lattice Relaxation Time (T_1) of Carbon ^{13}C Nuclei in the Methyl, Methine and Methylene Groups of SPP Samples A (Quenched from the Melt at 0 °C and Kept at 0 °C for 2 Months), Sample B (Sample A Annealed for 1 h at 70 °C), and Sample C (Sample A Annealed for 1 h at 90 °C)^a

carbon type	CS (ppm)	phase and conformational environment	T_1 (^{13}C) ^a					
			sample A	sample B (sample A annealed for 1 h at 70 °C)		sample C (sample A annealed for 1 h at 90 °C)		
CH ₃	19.7	mesophase + Am ^b (TTTT)	1.1	1.2		0.7		
	21.6	form I (TTGG)	0.8	0.7		0.6		
CH	27.3	form I (TTGG)		30.8 (76%)		29.9 (80%)		
	28.1	mesophase + Am (TTTT)	27.9 (67%)	4.0 (33%)	4.9 (34%)	4.9 (20%)		
CH ₂	40.3	form I (TTGG)	n.d. ^c	35.0 (41%)		35.6 (59%)		
	44.8	Am (TXYG)	3.8	36		41.1		
	48.9	form I (TTGG)		8.2				
	49.1	mesophase + Am (TTTT)	30.4 (65%)	3.7 (35%)	35.3 (68%)	3.5 (32%)	58.3 (72%)	3.4 (28%)
	50.2	(Am + interphase) ¹⁷ (TTTT)					25.4 (76%)	1.1 (24%)

^a The ^{13}C T_1 values were determined in a nonlinear least-squares fit of the peak intensities in ^{13}C CPMAS spectra obtained using the method developed by Torchia¹⁶ using almost 16 experimental points. For the resonances where a single T_1 value is determined, a single exponential function was used in the fit; for the resonances where two values of T_1 are indicated, the sum of two exponent function (the preexponential factors being enclosed in parentheses) were used. ^b Am: amorphous phase. ^c n.d.: not determinable.

Experimental Section

The syndiotactic polypropylene was synthesized as previously reported.¹⁵ The fraction of pentads measured by ^{13}C NMR was as follows: [rrrr] 85%, [rrmr] 1.4%, [mmrr] 3.3%, [rmrr] 2.4%, [rmm] 0.6%, [rrrm] 0.75%.

Polymer powders were melted in a hot press, at 150 °C, forming a film 0.10 mm thick, and rapidly quenched at 0 °C in an ice–water bath. The X-ray diffraction patterns, of small stripes of the film, extracted from the bath every 2 weeks, were monitored. The crystallization of the normal helical form occurring at room temperature is almost fully inhibited only after a permanence time of the film at 0 °C for 2 months.

X-ray powder spectra were recorded at room temperature with a Philips diffractometer using Ni-filtered Cu K α radiation.

Magic angle spinning (MAS) ^{13}C NMR spectra with cross polarization (CP) were measured at room temperature on a Bruker CXP 300 spectrometer operating at 75.5 MHz. The samples were spun in zirconia rotors at a rate of 4.5 kHz. The best CP contact time, regulated in order to maximize the signals of the nuclei in the rigid regions of the samples, was found 2 ms. A high-power proton decoupling (DD) field of 15G was applied. The delay between pulses was 5s. The resolution was checked on glycine (width at half-height = 26 Hz). Crystalline polyethylene was taken as an external reference at 33.63 ppm from tetramethylsilane (TMS). The values of the spin–lattice relaxation time T_1 of the ^{13}C nuclei were determined in a nonlinear least-squares fit of the peak intensities in ^{13}C CPMAS spectra, obtained through the method developed by Torchia,¹⁶ using almost 16 experimental points. The T_1 values of the ^{13}C nuclei for the examined samples are reported in Table 1. For the resonances where the peak intensity in the ^{13}C CPMAS spectra was fitted using the sum of two exponential functions, the relative contribution of the two functions is indicated. These values should not be taken as indicative of the relative content of the slowly and rapidly relaxing nuclei in the sample, since the experimental conditions (CP contact time, delay time between pulses) were settled to maximize the slowly relaxing nuclei contributions.

The infrared spectra were obtained by using a FTIR–Bruker IFS66 spectrophotometer with a resolution of 4 cm^{−1} (32 scans collected).

The transport properties were measured at 25 °C by a microgravimetric method, using a quartz spring balance having an extension of 16 mm/mg. Sorption was measured as a function of vapor activity $a = p/p_0$, where p is the actual pressure to which the sample was exposed and p_0 the saturation pressure at the temperature of the experiment. The vapor was dichloromethane at different activities, between 0.2 and 0.6.

Results and Discussion

Figure 1 plots the solid state ^{13}C NMR CP-MAS spectra recorded at room temperature of the sPP sample

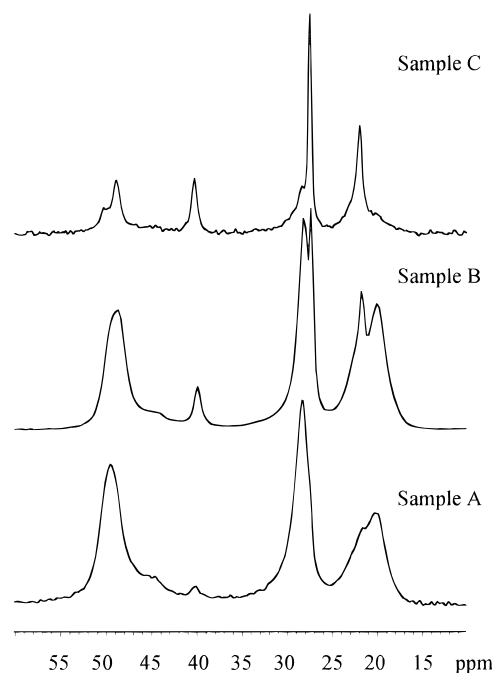


Figure 1. 75.5 MHz ^{13}C CP MAS spectra of the sPP sample quenched from the melt at 0 °C and kept at 0 °C for 2 months (sample A), sample A annealed at 70 °C for 1 h (sample B), and sample A annealed at 90 °C for 1 h (sample C).

quenched in ice–water from the melt at 150 °C and kept at 0 °C for 2 months (sample A), of the sample A after annealing for 1 h at 70 °C (sample B) and of the sample A after annealing for 1 h at 90 °C (sample C). In the CP-MAS spectrum of sample A the strong signals centered at 49.1, 28.1, and 19.7 ppm are relative to carbon nuclei belonging to the methylene, methine, and methyl groups, respectively, in an all-trans conformational sequence.^{17,18} The presence of additional weak signals around 44.8 ppm (which appears as a shoulder of the broad band occurring at 49.1 ppm) and at 40.3 and at 21.6 ppm (the shoulder of the broad band occurring at 19.7 ppm) indicate that a small amount of nuclei in a TX.YG (GX.YT, where the dots identify the position of the carbon nuclei in a CH₂ group and X and Y stand for the G or T states) conformational environments and in a G₂T₂ helical conformation are also present.^{18,19}

The spin–lattice relaxation times (T_1) of the ^{13}C nuclei giving rise to the above quoted resonances are reported

in Table 1. Corresponding to the resonances at 49.1 (CH_2 region) and 28.1 ppm (CH region), it is apparent the presence of a large component ($\approx 65\%$) showing T_1 values on the order of 30 s, indicating that a large amount of the nuclei contributing to these resonances under the chosen experimental conditions are embedded in rigid portions of the material, where long strands of chains are in an all *trans*-planar conformation; the remaining 35% of the nuclei contributing to the resonances at 49.1 ppm and 28.1 ppm under the chosen experimental conditions belongs to the amorphous phase (the T_1 relaxation times of them being on the order of a few seconds). The methyl carbon atoms, instead, owing to their characteristic mobility around the C–C bond, show values of T_1 on the order of 1 s, regardless of the rigidity of the host phase.¹⁸ Finally, the carbon nuclei giving rise to the resonances at 44.8, 40.3, and 21.6 ppm belong to mobile regions of the sample (T_1 relaxation times on the order of 4 s) which are probably amorphous or located at the interphase between the rigid and the amorphous phase. It is worth noting that the ^{13}C NMR CPMAS spectrum of sample A is similar to that one reported in the literature recorded in analogous conditions, relative to sPP stretched samples suitably prepared in the *trans*-planar form (form III).¹⁷

Upon thermal treatments, sample A is subjected to a phase transition to the helical forms of sPP, leading to a progressive increase of the signals at 48.9, 40.3, 27.3, and 21.6 ppm with the increase of the annealing temperature. We recall, indeed, that the signals at 48.9 and 40.3 ppm have been attributed to CH_2 carbon nuclei in the TG.GT and GT.TG conformational environments respectively, whereas the resonances at 27.3 and at 21.6 are relative to carbon nuclei belonging to methine and methyl groups in a TT.GG (and GG.TT) conformational environment, respectively.¹⁸ A large portion of the nuclei giving rise to these resonances are embedded in rigid (crystalline) portions of the material with chains in a helical T_2G_2 conformation (see Table 1 for the T_1 values). In the case of sample B large and strong bands centered at 49.1 and 19.7 ppm and a narrow signal at 28.1 ppm are still present; they are relative to CH_2 , CH_3 , and CH carbon atoms, respectively, belonging to a rigid phase containing long portions of chains in *trans*-planar conformation (correspondingly, the T_1 values are on the order of 30–35 s for the CH_2 and the CH carbon atoms; see Table 1). In the case of sample C, the amount of this *trans*-planar rigid phase is noticeably reduced (see for instance the small shoulder at 27.3 ppm for the methine carbon atom) and the sample results in a large amount crystallized in a more stable helical crystalline form. From the ^{13}C NMR analysis alone, it is not possible to establish the nature of this helical crystalline forms (form I, form II, or both). This question will be addressed by the X-ray diffraction analysis in the following.

As a further check of the chain conformation in the rigid phase of sample A, in Figure 2 the FTIR spectrum of this sample ($1600\text{--}700\text{ cm}^{-1}$) is reported in absorbance and compared with the spectrum of sample C. We observe that the bands of the helical form of sPP,²⁰ appearing at 810, 868, 977, and 1005 cm^{-1} are strongly reduced or completely absent. At variance, bands corresponding to long polymer strands in a *trans*-planar conformation²¹ at 831, 963, and 1140 cm^{-1} , not present in samples crystallized in the helical forms, are here

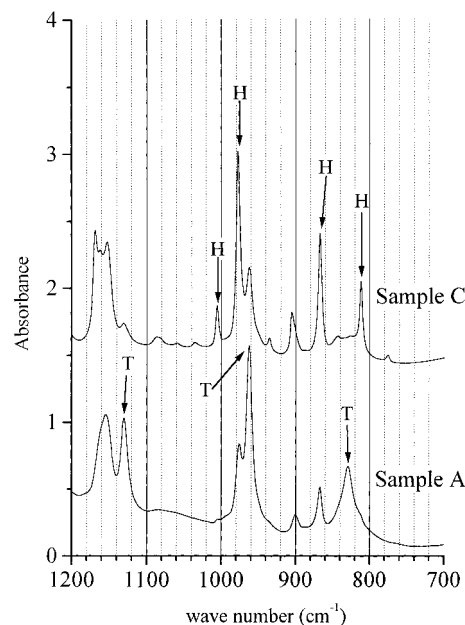


Figure 2. FTIR spectra of sPP samples A and C. The arrows point to the IR bands relative to long strands of chains in the helical T_2G_2 conformation (H) and in the *trans*-planar conformation (T).

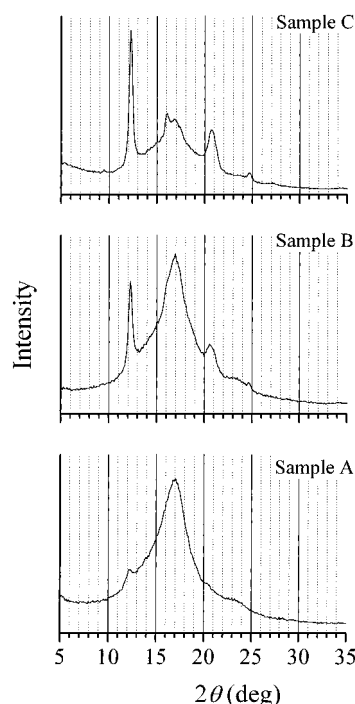


Figure 3. X-ray diffraction profiles of sPP samples A, B, and C (Ni-filtered $\text{Cu K}\alpha$).

very evident and well developed. This result confirms that the chains, in the sample held for at least 2 months in the cold bath, assumed a prevalently zigzag conformation.

In Figure 3 the X-ray diffraction pattern of the sPP samples A, B, and C are compared. For the sample A, a broad halo centered around $2\theta = 17^\circ$ ($\text{Cu K}\alpha$) together with a smaller one centered at $2\theta = 24^\circ$ is apparent; also, a small maximum around $2\theta = 12.3^\circ$ ($\text{Cu K}\alpha$) is present, probably relative to a helical crystalline form produced at room temperature upon removing the sample from the bath at 0°C . This pattern closely correspond to that one already reported by Nagaoki et

al. (Figure 3 of ref 14) for a sPP sample prepared in analogous conditions. As already noticed by the authors of ref 14, the X-ray diffraction pattern of sample A in Figure 3 does not correspond to that one of the amorphous phase of sPP neither to that one of any of the known crystalline helical forms of sPP (forms I, II, and IV).^{8,10} Also, as already discussed in the Introduction, it may not correspond to the X-ray diffraction pattern of a powder in the *trans*-planar form (form III),⁹ even if very small dimensions of the crystals are supposed, although the ¹³C NMR CP MAS and FTIR spectra of this sample (see Figures 1 and 2) reveal that the sPP stretches embedded in the rigid regions are prevailing in a *trans*-planar conformation. The X-ray diffraction pattern of Figure 3 indicates that a novel form of sPP is obtained, when the samples are quenched from the melt at 0 °C and kept in the cold bath for a long enough time. This new phase can be rather identified as a mesophase or a paracrystalline highly disordered phase with chains in *trans* planar conformation.

The annealing of sample A at 70 °C (sample B) and at 90 °C (sample C) produces a crystallization of the helical forms and probably also a gradual transformation of the mesophase into a more stable helical form. From the analysis of the diffraction patterns of the annealed samples (Figure 3) it is possible to establish that the form I is mostly produced upon the thermal treatment of the mesophase. In the case of sample B and sample C, indeed, diffraction maxima at $2\theta = 12.3$, 15.8 (apparent as a shoulder in the X-ray diffraction pattern of sample B, in Figure 3), and 20.6° (Cu K α) become increasingly narrow and sharp with the increasing of the annealing temperature, whereas the height of the diffraction maximum centered around $2\theta = 17^\circ$ (Cu K α), decreases. The latter maximum at $2\theta = 17^\circ$ is still present in the case of sample B and appears as a shoulder in the case of sample C. This could also indicate a partial transformation of the mesophase into form II,⁸ but the results of our solid state ¹³C NMR analysis indicate that a not negligible amount of the mesophase with chains in a *trans*-planar conformation is still present. It is worth noting that the annealing of sample A does not affect the half-height width of the diffraction peak at $2\theta = 17^\circ$; were this sample crystallized in form III with reduced dimensions of the crystallites one should expect a narrowing of the diffraction peaks as a consequence of annealing procedures. The rather constancy of the broadness of the halo at $2\theta = 17^\circ$ with the annealing temperature is a further indication that this novel form of sPP should be more correctly identified as a mesophase.

To quantitatively measure the amount of this new (rigid) phase (mesophase) in sample A, we performed measurements of the transport properties of vapors at low activity. The transport properties of a given polymeric material, indeed, are strongly influenced by the relative mobility of the chain molecules embedded in the various phases. The rigid regions, usually crystalline, are generally impermeable to the gases and vapors at low activity ($a < 0.4$). At a given activity of the vapor, one can write:²²

$$c_{eq} = c_{eq}(\text{amorphous sample}) (1 - \alpha_c)$$

$$\alpha_a = (1 - \alpha_c)$$

$$c_{eq}(\text{amorphous sample}) = c_{eq}/\alpha_a$$

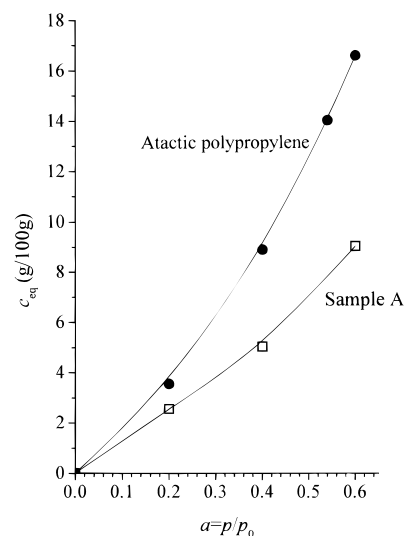


Figure 4. Equilibrium concentration of dichloromethane vapors (c_{eq}) in sample A and in an amorphous (atactic) polypropylene sample as a function of vapor activity (a) measured at room temperature. p is the actual pressure to which the sample is exposed and p_0 the saturation pressure at the temperature of the experiment.

where c_{eq} is the equilibrium concentration of vapor in the sample at a given activity, α_a and α_c are the fractions of the permeable (amorphous) and impermeable phases, respectively and c_{eq} (amorphous sample) is the equilibrium concentration of a completely amorphous sample. Therefore, sorption of a biphasic sample compared to the sorption of a completely amorphous sample, gives α_a . It is worth noting that this method can be used even when the sample contains a mesophase, since generally also the mesophases are impermeable to the vapor at low activity.²² As for the sorption of the amorphous sample, in our case, because it is not possible to obtain amorphous syndiotactic polypropylene, we can refer to the sorption at low activity of atactic polypropylene. This assumption was found valid in the case of isotactic polypropylene of different crystallinities.²³

In Figure 4 the equilibrium concentration c_{eq} (grams of vapor per 100 g of dry polymer) is reported for atactic polypropylene and for the sPP sample A, as a function of the vapor activity. At each vapor activity the sorption of the latter sample is lower than that of atactic polypropylene; from the ratio of the sorption we derived the value of α_a of 78%, giving a fraction of impermeable phase (mesophase) of 22%.

The results reported in this paper indicate that a new phase of sPP can be stabilized at low temperature following the procedure described by Nakaoki et al.¹⁴ This new phase is characterized by chains in *trans*-planar conformation but cannot be identified as the known crystalline form III of sPP. It should be rather identified as a mesophase, or also paracrystalline, disordered phase, containing lateral disorder in the packing of *trans*-planar chains. We have shown that this phase is rather stable up to 80 °C, whereas at 90 °C, it is almost completely transformed into the more stable form I.

Acknowledgment. This work was supported by the Ministero dell'Università e della Ricerca Scientifica e Tecnologica (PRIN 1998 titled "Stereoselective Polymerization: New Catalysts and New Polymeric Materials").

References and Notes

- (1) Natta, G.; Corradini, P.; Ganis, P. *Makromol. Chem.* **1960**, *39*, 238.
- (2) Corradini, P.; Natta, G.; Ganis, P.; Temussi, P. A. *J. Polym. Sci., Part C* **1967**, *16*, 2477.
- (3) Natta, G.; Peraldo, M.; Allegra, G. *Makromol. Chem.* **1964**, *75*, 215.
- (4) Lotz, B.; Lovinger, A. J.; Cais, R. E. *Macromolecules* **1988**, *21*, 2375.
- (5) Lovinger, A. J.; Lotz, B.; Cais, R. E. *Polymer* **1990**, *31*, 2253.
- (6) Lovinger, A. J.; Davis, D. D.; Lotz, B. *Macromolecules* **1991**, *24*, 552.
- (7) Lovinger, A. J.; Lotz, B.; Davis, D. D.; Padden, F. J. *Macromolecules* **1993**, *26*, 3494.
- (8) De Rosa, C.; Corradini, P. *Macromolecules* **1993**, *26*, 5711.
- (9) Chatani, Y.; Maruyama, H.; Naguchi, K.; Asanuma, T.; Shiomura, T. *J. Polym. Sci., Part C* **1990**, *28*, 393.
- (10) Chatani, Y.; Maruyama, H.; Asanuma, T.; Shiomura, T. *J. Polym. Sci., Polym. Phys.* **1991**, *29*, 1649.
- (11) De Rosa, C.; Auriemma, F.; Vinti, V. *Macromolecules* **1997**, *30*, 4137.
- (12) De Rosa, C.; Auriemma, F.; Vinti, V. *Macromolecules* **1998**, *31*, 7430.
- (13) Lotz, B.; Mathieu, C.; Thierry, A.; Lovinger, A. J.; De Rosa, C.; Ruiz de Ballesteros, O.; Auriemma, F. *Macromolecules* **1998**, *31*, 9253.
- (14) Nakaoki, T.; Ohira, Y.; Hayashi, H.; Horii, F. *Macromolecules* **1998**, *31*, 2705.
- (15) Guadagno, L.; Fontanella, C.; Vittoria, V.; Longo, P. *J. Polym. Sci.: Polym. Phys.* **1999**, *37*, 173.
- (16) Torchia, D. A. *J. Magn. Reson.* **1978**, *30*, 613.
- (17) Sozzani, P.; Galimberti, M.; Balbontin, G. *Makromol. Chem. Rapid Commun.* **1992**, *13*, 30.
- (18) Sozzani, P.; Simonutti, R.; Comotti, A. *Magn. Res. Chem.* **1994**, *32*, S45.
- (19) Sozzani, P.; Simonutti, R.; Galimberti, M. *Macromolecules* **1993**, *26*, 5782.
- (20) Natta, G.; Pasquon, I.; Corradini, P.; Peraldo, M.; Pegoraro, M.; Zambelli, A. *Rend. Accad. Naz. Lincei* **1960**, *28*, 539.
- (21) Natta, G.; Peraldo, M.; Allegra, G. *Macromol. Chem.* **1964**, *75*, 215.
- (22) Rogers, C. E. *Polymer Permeability*; Comyn, J., Ed.; Elsevier: Belfast, Northern Ireland, 1985.
- (23) D'Aniello, C.; Guadagno, L.; Gorrasi, G.; Vittoria, V. *Polymer*, in press.

MA000373K